Electron density and temperature measurements in a laser produced carbon plasma

S. S. Harilal, C. V. Bindhu, Riju C. Issac, V. P. N. Nampoori, and C. P. G. Vallabhan[a)]
Laser Division, International School of Photonics, Cochin University of Science & Technology, Cochin 682 022, India

(Received 10 March 1997; accepted for publication 13 May 1997)

Plasma generated by fundamental radiation from a Nd:YAG laser focused onto a graphite target is studied spectroscopically. Measured line profiles of several ionic species were used to infer electron temperature and density at several sections located in front of the target surface. Line intensities of successive ionization states of carbon were used for electron temperature calculations. Stark broadened profiles of singly ionized species have been utilized for electron density measurements. Electron density as well as electron temperature were studied as functions of laser irradiance and time elapsed after the incidence of laser pulse. The validity of the assumption of local thermodynamic equilibrium is discussed in light of the results obtained. © *1997 American Institute of Physics.* [S0021-8979(97)04116-9]

I. INTRODUCTION

Pulsed laser induced plasma has a very short temporal existence and is transient in its nature, with a fast evolution of the characteristic parameters that are heavily dependent on irradiation conditions such as incident laser intensity, irradiation spot size, ambient gas composition and pressure. It is also true that these parameters vary drastically with axial or radial distance from the target surface under the same irradiation conditions. Detailed investigation of the optical emission of the plasma plume gives information on the spatial and temporal evolution of transient species produced during laser–target interaction, such as excited atoms, ions or molecules.[1] The spectroscopic studies made on spatial volume elements in the neighborhood of the target surface in the early stages of the plasma evolution give direct information about the laser–target interaction as well as laser–plasma interaction. Investigation of optical emission at comparatively larger distances from the target surface results in yielding information on the plasma species reactivity, which is an important quantity needed to maintain quality of thin films prepared using the pulsed laser deposition technique. It also reveals the dynamics of the ablated material before collision with a substrate surface.[2,3]

Laser induced graphite plasma has several applications. Carbon thin films have been attracting both intensive theoretical and experimental investigation due to their diamond-like properties.[4–8] This technique is also utilized for fullerene synthesis in an ambient gas.[9–11] It is a potential method for many possible new, yet to be defined technological applications. While this strong interest leads to intense research work on the physical and chemical properties of these classes of carbon, the precise nature of its formation remains controversial. Recent measurements performed over a wide range of expansion durations have demonstrated a complicated gas dynamic picture of plume ambient gas interaction, which is characterized by different propagation phases and is accompanied by plume oscillations at rather high background pressure.[12–14] However, relatively little quantitative information is available on either the fundamental graphite plasma parameters, like electron temperature, electron density etc., or on the nature of the dominant plume excitation processes in different spatial and temporal regions of the expanding plasma. Such data are required in order to develop and test models of plasma processes[15,16] and enable us to evaluate the energy transport into the plasma with regard to temporal and local behavior as well as its effectiveness.

There are several diagnostic techniques employed for the determination of electron density which includes, plasma spectroscopy,[17,18] Langmuir probe,[19,20] microwave and laser interferometry,[21–23] and Thomson scattering.[24,25] Thomson scattering is probably the most direct and least theory-dependent, while spectroscopy is the simplest as far as instrumentation is concerned. Plasma density determination using Stark broadening of spectral lines is a well established and reliable technique[17,26,27] in the range of number density 10^{14}–10^{18} cm^{-3}. The electron temperature is an equally important plasma parameter which can be determined spectroscopically in a variety of ways: from the ratio of integrated line intensities, from the ratio of line intensity to underlying continuum, and from the shape of the continuum spectrum.[17]

In this paper, we report the studies on plasma parameters such as electron density and electron temperature and their dependence on factors like incident laser irradiance, time after the elapse of laser pulse and spatial separation from the target surface. The relative line intensities of successive ionization stages of carbon atoms are used for the determination of electron temperature while Stark broadened profile of singly ionized carbon atom is used for the measurement of electron density.

II. EXPERIMENTAL SETUP

Details of the experimental technique are given elsewhere.[28] The plasma was generated by ablation of a high purity polycrystalline graphite sample using 1.06 μm radiation pulses from a Q-switched Nd:YAG laser with repetition rate 10 Hz (maximum pulse energy 275 mJ). The estimated

[a)]Electronic mail: root@cochin.ernet.in

 0021-8979/97/82(5)/2140/7/$10.00

laser spot size at the target was 200 μm. The target in the form of a disc (25 mm diameter and 5 mm thickness) is placed in an evacuated chamber provided with optical windows for laser irradiation and spectroscopic observation of the plasma produced from the target. During these studies the pressure inside the vacuum chamber is kept at $\sim 10^{-4}$ mbar. The target was rotated about an axis parallel to the laser beam to avoid nonuniform pitting of the target surface. The bright plasma emission was viewed through a side window at right angles to the plasma expansion direction. The section of the plasma was imaged onto the slit of a 1 m monochromator (Spex, model 1704, grating with 1200 grooves per mm blazed at 500 nm, maximum resolution 0.05 nm), with entrance and exit slits are kept parallel to the target surface, using appropriate collimating and focusing lenses so as to have one to one correspondence with the sampled area of the plasma and the image. The recording was done by using a thermoelectrically cooled Thorn EMI photo multiplier tube, which was coupled to a boxcar averager/gated integrator (Standford Research Systems, SRS 250). The averaged output from the boxcar averager was fed to a chart recorder, which for the present study averaged out intensities from 10 pulses. For Stark broadening studies, the resolution of the monochromator was kept at its maximum by keeping the entrance and exit slit widths at a minimum (3 and 6 μm).

III. RESULTS AND DISCUSSION

One of the most powerful spectroscopic techniques to determine the electron density with reasonable accuracy is by the measurements of the Stark broadened line profile of an isolated atom or singly charged ion.[17,29,30] For the estimation of electron density, the Stark broadened profile of C II transition at 392 nm ($3p^2p^0-4s^2S$) is charted keeping the monochromator at its maximum resolution. Three broadening mechanisms are likely to contribute significantly to linewidths observed in plasmas produced during pulsed laser ablation viz., Doppler broadening, resonance pressure broadening and Stark broadening. For ablation in vacuum, where ablated species exhibit high expansion velocities, one of the dominant contributions to spectral line broadening is Doppler broadening, which is due to different Doppler shifts (i.e., $\Delta\lambda=\lambda v_z/c$) experienced by the species in different regions of the plume having different velocity components v_z in the direction of observation. Since the expansion velocities of the C II ions are found[14] to be $\sim 10^6$ cm s^{-1}, which corresponds to Doppler linewidths full width half maximum (FWHM) ~ 0.13 A^0, the effect due to Doppler broadening can be ignored. The pressure broadening is proportional to the ground state number density of the corresponding species and transition oscillator strength. As only a small transition oscillator strength has been reported[17] for C II at 392 nm (0.134), the resonance broadening part can be safely neglected. Stark broadening of spectral lines in plasmas results from collisions with charged species resulting in both a broadening of the line and a shift in the peak wavelength.

The FWHM of the Stark broadened lines $\Delta\lambda_{1/2}$ is related to the electron density by the expression[17]

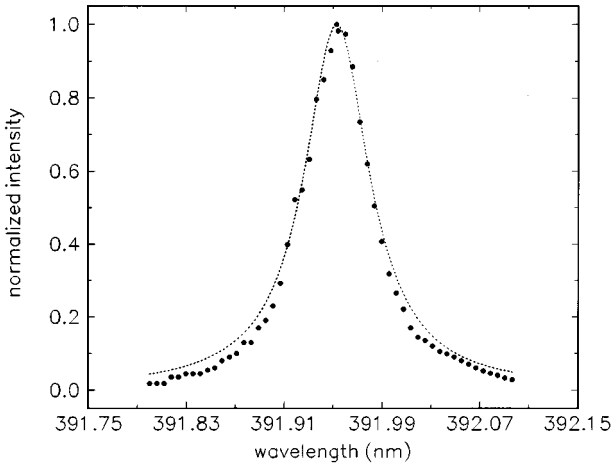

FIG. 1. Typical Stark broadened profile of C II transition ($3p^2p^0-4s^2s$) at 392 nm for 1.06 μm radiation at a distance 6 mm from the target. The dotted line represents the Lorentzian fit. Full width half maxima (FWHM) of these spectra were used for the estimation of electron density.

$$\Delta\lambda_{1/2}=2W\left(\frac{n_e}{10^{16}}\right)+3.5A\left(\frac{n_e}{10^{16}}\right)^{1/4}\times\left(1-\frac{3}{4}N_D^{-1/3}\right)W\left(\frac{n_e}{10^{16}}\right)A^0, \quad (1)$$

where W is the electron impact parameter which can be incorporated to different temperatures;[17] A is the ion broadening parameter, and N_D the number of particles in the Debye sphere. The first term on the right side of Eq. (1) represents the broadening due to electron contribution and the second term is the ion correction factor. For nonhydrogenic ions Stark broadening is predominantly by electron impact. Since the perturbations caused by ions is negligible compared to electrons, the ion correction factor can safely be neglected. Therefore Eq. (1) reduces to

$$\Delta\lambda_{1/2}=2W\left(\frac{n_e}{10^{16}}\right)A^0. \quad (2)$$

Typical Stark broadened line profile is approximately Lorentzian and the experimental results shown here in Figure 1 fits fairly well with a typical Lorentzian profile.

Relative line intensities from the same element and ionization state usually do not provide accurate temperatures. The principal reason for this is the relatively small separation between the upper levels of two lines. Considerable improvement in sensitivity can be obtained by selecting lines from successive ionization stages of the same element, because the effective energy difference is now enhanced by the ionization energy, which is much larger than the thermal energy. In local thermodynamic equilibrium (LTE), the ratio of such line intensities is given by[17]

$$\frac{I'}{I}=\left(\frac{f'g'\lambda^3}{fg\lambda'^3}\right)(4\pi^{3/2}a_0{}^3n_e)^{-1}\left(\frac{kT_e}{E_H}\right)^{3/2}$$
$$\times\exp\left(-\frac{E'+E_\infty-E-\Delta E_\infty}{kT}\right), \tag{3}$$

where the primed symbols represent the line of the atom with higher ionization stage, f is the oscillator strength, g is the statistical weight, a_0 is the Bohr radius, E_H is the ionization energy of the hydrogen atom, E the excitation energy, and ΔE_∞ is the correction to the ionization energy E_∞ of the lower ionization stage due to plasma interactions.

The correction factor in the ionization energy is given by

$$\Delta E_\infty=3z\frac{e^2}{4\pi\epsilon_0}\left(\frac{4\pi n_e}{3}\right)^{1/3}, \tag{4}$$

where $z=2$ for the lower ionization state.

For the evaluation of T_e we make use of line intensities corresponding to the lines at 464.7 nm and 569.6 nm of C III and 392 nm and 407.4 nm lines of C II. The spectroscopic constants of these spectral lines are taken from Ref. 17.

A. Spatial dependence

The plasma represents a heated high pressure gas kept in a region of small dimensions which later on, is allowed sudden expansion into the surrounding vacuum. In a laser produced plasma the preferential vaporization of the evaporated material is always found to be in a direction perpendicular to the target surface, irrespective of the angle of incidence of laser beam. Measurements were performed in carbon plasma generated in these experiments at different distances and various irradiance levels. Line shape analyses were repeated at different distances from the target surface which provides a direct indication of space evolution of electron density giving an insight into the basic ionization processes taking place in the pulsed laser ablation.

When the laser is focused onto the carbon target, which is placed in a vacuum due to density gradients in the plasma, a rapid expansion takes place. The estimations of electron temperature and density of the laser produced carbon plasma were carried out here for distances up to 12 mm from the target surface in a time integrated manner. The spatial dependence of electron temperature and electron density of the carbon plasma are given in Figures 2 and 3. The temperature and density show a decreasing behavior with distance. With increasing separation from the target surface, the electron temperature falls from 2.43 eV at 1 mm to 1.6 eV at 11 mm while electron density decreases from 2.1×10^{17} cm^{-3} at 1 mm to 1×10^{17} cm^{-3} at 11 mm. These results are consistent with the recently reported values of such quantities.[31,32]

The variation of electron temperature with distance (z) perpendicular to the target surface shows a $z^{-0.1}$ dependence. For these studies time integrated intensities were used and the value of T_e presented at different distances from the target should be regarded as indicative of the average conditions occurring in an Nd:YAG laser induced carbon plasma, rather than defining the conditions at a particular stage of its evolution.

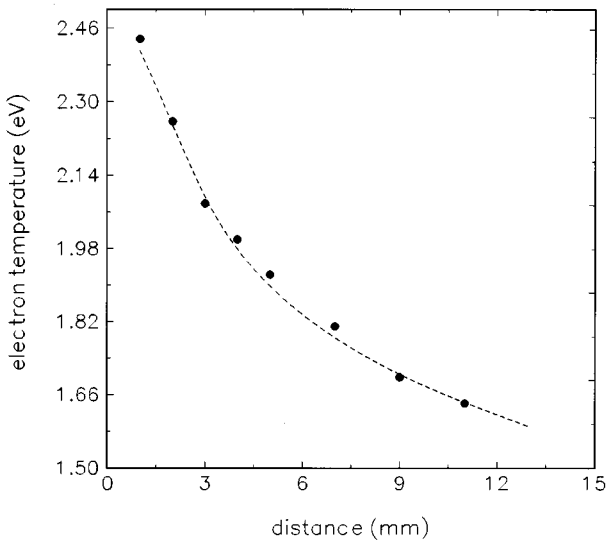

FIG. 2. The variation of electron temperature as a function of distance (z) from the target surface. The dotted line represents $z^{-0.1}$ fit (laser irradiance used 50 GW cm^{-2}).

The density gradients of the plasma at a point z at any time t can be expressed as[33,34]

$$n_e(z,t)=n_0(t)\left(1-\frac{z}{Z(t)}\right), \tag{5}$$

where n_0 is the density at the center of the laser irradiated spot ($z=0$) at time t, the z coordinate is directed perpendicular to the target and $Z(t)$ refer the spatial coordinate of the leading edge of the plasma.

According to Eq. (5), the electron density decreases linearly with distance from the target surface. However, in actual practice the density gradient does not decrease linearly. The variation of n_e as a function of distance follows approximately a $1/z$ law at short distances, indicating that the initial

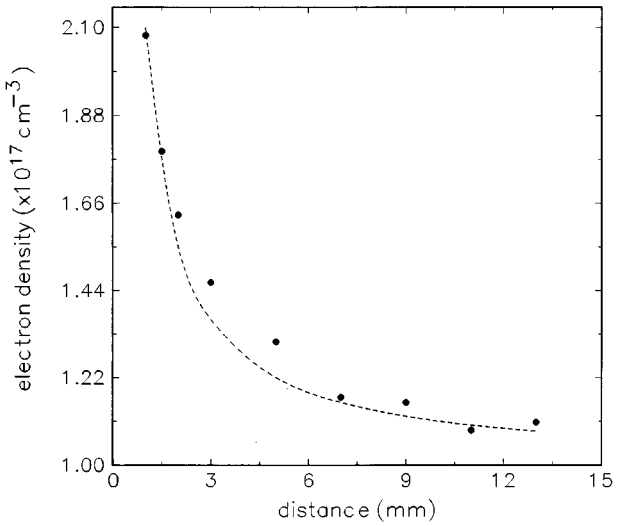

FIG. 3. Electron density of the graphite plasma as a function of distance from the target surface. The dotted line represents $1/z$ curve (laser irradiance used 50 GW cm^{-2}).

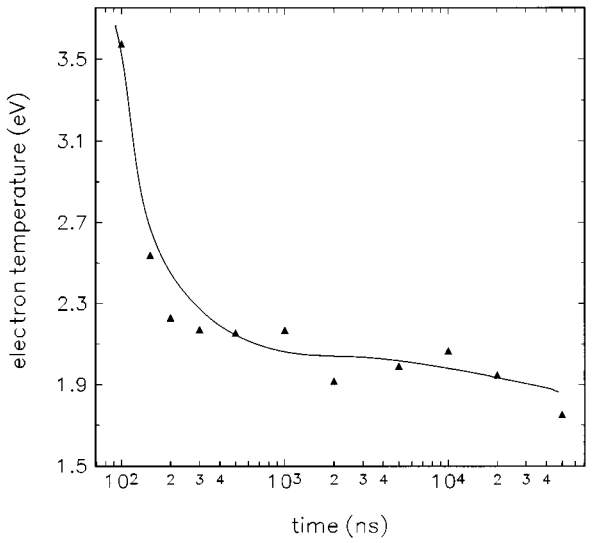

FIG. 4. Electron temperature of the expanding plasma as a function of time (distance 3 mm; laser irradiance 50 GW cm^{-2}).

expansion of the electron gas is one dimensional, in good agreement with the predictions of the plume expansion model given by Singh and Narayan.[34]

B. Time dependence

The temporal evolution of electron temperature and electron density are of prime importance, since many kinetic reaction rates depend directly or indirectly on these parameters. The experimentally measured variations of temperature and density of the laser generated carbon plasma with time are given in Figures 4 and 5, respectively. For these studies the boxcar gate width was set at 10 ns. An initial electron temperature of about 3.6 eV and density of about 4×10^{17} cm^{-3} were observed.

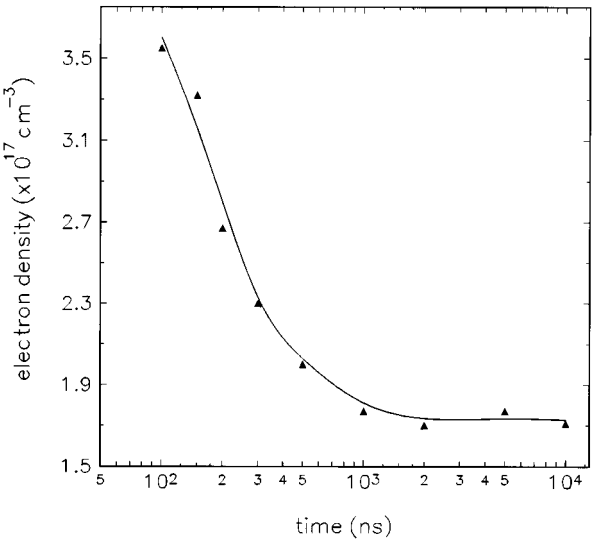

FIG. 5. Electron density of the expanding plasma as a function of time (distance 3 mm; laser irradiance 50 GW cm^{-2}).

At shorter times ($<$ 100 ns), the line to continuum ratio is so small and the temperature measurement is very sensitive to errors in setting the true continuum level. This problem is particularly acute for time up to 100 ns. For times >100 ns, the line to continuum ratios are within reasonable limit, interference with the continuum measurement is not severe and the values of T_e shown in the figure should be reliable.

Initially the plasma expands isothermally within the time of the duration of the laser pulse. After the termination of the laser pulse, the plasma expands adiabatically.[33] During this expansion the thermal energy is converted into kinetic energy and the plasma cools down rapidly. An adiabatic expansion of the plasma occurs, when the temperature can be related to the dimensions of the plasma by the adiabatic thermodynamic relation

$$T[X(t)Y(t)Z(t)]^{\gamma-1}=\text{constant}, \tag{6}$$

where γ is the ratio of specific heat capacities at constant pressure and volume, $X(t)$, $Y(t)$ and $Z(t)$ are the dimension of the expanding plasma in the three mutually orthogonal directions.

It is noted that within 300 ns after the laser pulse the temperature drops from 3.6 eV to 2.2 eV while the density falls from 3.6×10^{17} cm^{-3} to 1.5×10^{17} cm^{-3}. In the early stages of plasma evolution the electron temperature is high and it varies very rapidly. When the time is greater than 300 ns, the electron temperature of the plasma is reduced to about $\sim$ 2 eV. But afterwards the temperature gets stabilized for a period up to $\sim$ 2000 ns. As seen from the adiabatic equation of state, the rate of decrease of temperature strongly depends on the specific heat ratio γ. However, in actual practice (as shown in Figure 3) the temperature decreases more slowly than predicted by the adiabatic equation due to preferential expansion of the plasma in one dimension during initial stages. But, 300 ns after the initiation of the plasma the temperature begins to decrease more slowly due to the energy released by the recombinations which compensate the cooling due expansion processes. The variation of electron temperature with time (t) for 1.06 μm radiation shows t^{-2} dependence which is in accordance with the theoretical adiabatic expansion model by Rumsby and Paul.[35] The electron density has been found to decay with a dependence $n_e \propto t^{-2}$ rather than the reported theoretical $n_e \propto t^{-3}$. Such discrepancies from the t^{-3} has been noted by others also.[35]

C. Effect of laser irradiance

The nature and characteristics of the laser produced plasma strongly depend on the laser irradiance. Figures 6 and 7 give variation of electron temperature and density of the laser produced graphite plasma with respect to laser irradiance at a distance 3 mm from the target surface. Time integrated line intensities were used for these calculations. As laser irradiance increases from 21 GW cm^{-2} to 64 GW cm^{-2}, the electron temperature increases from 1.29 eV to 2.15 eV, and saturates at higher irradiance levels, while electron densities vary from 1×10^{17} cm^{-3} to 1.6×10^{17} cm^{-3} and then saturate. The saturation in T_e and n_e at higher irradiance conditions is expected to be due to plasma shielding,

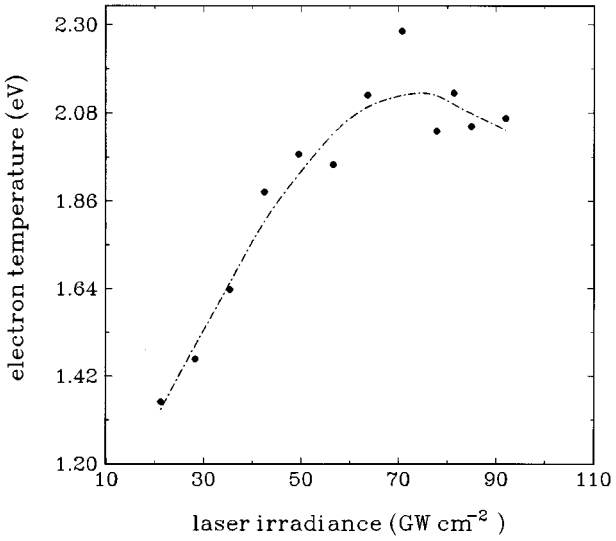

FIG. 6. The variation of electron temperature with laser irradiance (distance 3 mm).

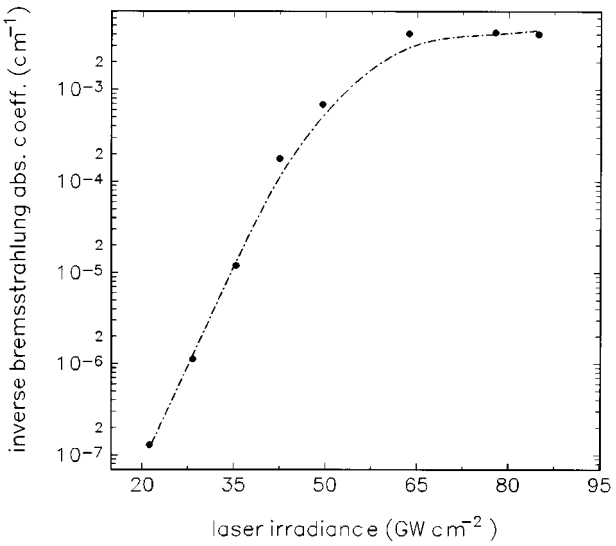

FIG. 8. The estimated absorption depth (at 1.06 μm) of graphite vapor plume for inverse bremsstrahlung.

i.e., absorption and/or reflection of the laser photons by the plasma itself.[36] The reflection of the incident laser photon depends on the plasma frequency ν_p, which should be lower than the laser frequency. For the Nd:YAG laser, its fundamental wavelength (1.06 μm) corresponds to a frequency $\nu_l = 2.828\times10^{14}$ Hz. The plasma frequency is given by $\nu_p = 8.9\times10^3 n_e^{0.5}$, where n_e is the electron density. Calculations show that with $n_e \sim 10^{17}$ cm^{-3}, $\nu_p = 6.5\times10^{12}$ Hz, which is much smaller than the laser frequency. So the energy losses due to reflection of Nd:YAG laser beam from the plasma can be assumed to be insignificant.

The two dominant mechanisms responsible for plasma absorption at these laser irradiance levels used in our work are inverse bremsstrahlung and photoionization. Inverse bremsstrahlung absorption α_{ib} via free electrons is approximated by[30]

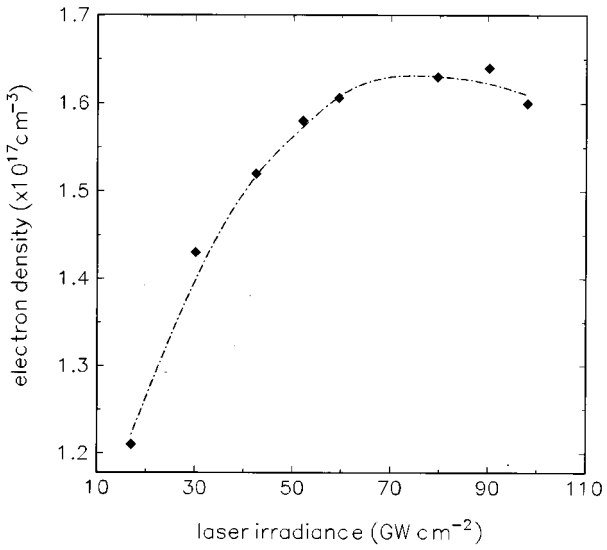

FIG. 7. The variation of electron density with laser irradiance (distance 3 mm).

$$\alpha_{ib}(\mathrm{cm}^{-1}) = 1.37\times10^{-35}\lambda^3 n_e^2 T_e^{1/2}, \tag{7}$$

where λ is the wavelength of the laser photons in μm. The absorption due to inverse bremsstrahlung at different laser irradiance levels is shown in Figure 8. It is noted that the absorption due to inverse bremsstrahlung is negligibly small at low irradiance levels and increases exponentially with increasing laser irradiance and saturates at higher irradiance levels.

Absorption via photoionization can be estimated with Kramer's formula and absorption coefficient[37,38]

$$\alpha_{pi} = \sum_n 7.9\times10^{18}\left(\frac{E_n}{h\nu_l}\right)^3\left(\frac{1}{E_n}\right)^{1/2} N_n, \tag{8}$$

where E_n and N_n are the ionization energy and number density of the excited state n; h is Plank's constant, ν_l is laser frequency; I is ionization potential of the ground state atom. The absorption coefficient of photoionization is obtained by summing up all the excited states whose ionization energies are smaller than the laser photon energy. Since the excitation potentials of atomic transitions of carbon atoms are much greater than the photon energy of the pump used (1.17 eV), direct photoionization by the absorption of a laser photon is ruled out. The only possibility for this type of ionization to happen is by the simultaneous absorption of a number of photons.

The ionization rate in the case of photoionization is given by[39]

$$W_n = \omega_0 n_e^{3/2}\left(\frac{\xi_{os}}{I_i}\right)^p, \tag{9}$$

where $p = I_i/\hbar\omega_0$ is the number of photons absorbed and ξ_{os} is the electron oscillation energy which is given by

$$\xi_{os} = 0.093\lambda^2 I(\mathrm{eV}), \tag{10}$$

where I is the power density used for the ablation (W cm^{-2}). Since the ionization rate depends on number of

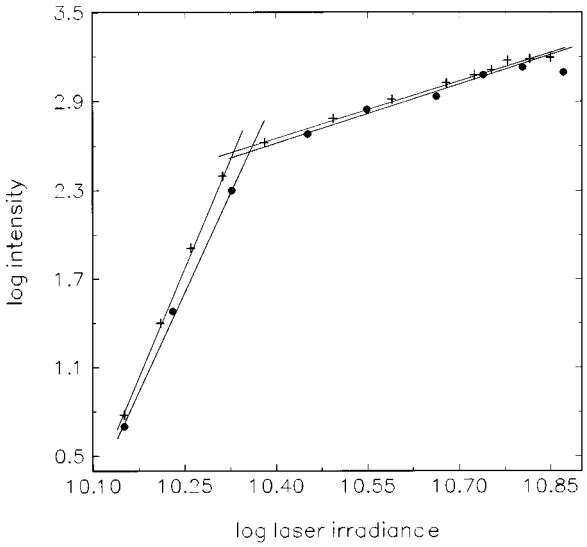

FIG. 9. Variation of logarithm of the ion emission intensity of singly and doubly ionized species of carbon with laser irradiance. (+) C II transition ($3p^2p^0-4s^2S$) at 392 nm and (●) C III transition ($3p^1P^0-3d^1D$) at 580.1 nm.

absorbed quanta p and the laser irradiance through ξ_{os}, the slope of the log–log plot between laser irradiance and emission intensity will be a direct measure of the number of photons involved in this process. Figure 9 gives such a plot for C II and C III ionic species from the laser produced carbon plasma. One can see that the intensity of the line grows as I^p, where $p = 10$ for C II and $p = 9$ for C III, which are in good agreement with the photon energy used in the present experiment and the first ionization potential of carbon atoms (11.3 eV). The mismatch observed in the case of C III ions implies that along with photoionization, other processes like impact ionization and direct generation of the species at higher energy states also take place and these processes may be more predominant in the present case. At higher irradiance levels the exponent is close to unity and obviously the multiphoton ionization is not a dominant process in this regime. Besides photoionization, other mechanisms especially impact ionization, thermal ionization, etc. may also affect the absorption coefficient of the plasma.

The saturation in T_e and n_e at higher irradiance levels cannot be explained by considering only the prominent absorption mechanisms via inverse bremsstrahlung and photoionization. Such temperature and density behavior can be explained by assuming the formation of a self regulating regime at higher irradiances.[34,40] During the incidence of the laser pulse on the target surface, we can have four separate domains which include:

(i) unaffected bulk target,
(ii) evaporating target surface,
(iii) area near the target absorbing the laser beam, and
(iv) rapidly expanding outer edge of the plasma which is transparent to the laser beam.

During isothermal expansion a dynamical equilibrium exists between the plasma absorption coefficient and rapid transfer of thermal energy into kinetic energy, which controls the isothermal temperature of the plasma. At high irradiance levels, when an appreciable amount of energy is absorbed by the plasma, a self regulating regime may form near the target surface. If the absorption of the laser photons by the plasma becomes higher due to high plasma density, the evaporation of the species from the target becomes less, which in turn decreases density of the charged species. This consequently increases the absorption of the laser photons by the target, which in turn increases the temperature of the plasma. On the other hand, when the absorption of the laser energy is less the process is reversed with similar results. It has been theoretically proved that[41] the density, temperature and dimensions of the plume adjust in such a manner that the plasma absorbs the same amount of laser radiation to maintain a self regulating regime. This assumption was found to be valid in laser generated plasma, where thermalization time is significantly less than the plasma expansion time, resulting in an establishment of uniform temperature in the plasma. The thermalization time τ_{ei} of energy exchange between electron and ions during collision can be estimated from the relation[37]

$$\tau_{ei}=\frac{252MT_e^{3/2}}{\ln(\Lambda)n_e}, \tag{11}$$

where

$$\Lambda=\frac{3(kT)^{3/2}}{4(\pi n_e)^{1/2}e^3}, \tag{12}$$

where $\ln\Lambda$ stands for the Coulomb logarithm, which involves dynamical information about ion-electron collisions, M is atomic weight. With $n_e=10^{17}$ cm^{-3}, $T_e\approx T$ (vapor temperature) = 22 000 K, the relaxation time is $\sim$ 3 fs, which is much smaller than the expansion time or pulse width of the laser beam which is of the order of few of nanoseconds.

D. Local thermodynamic equilibrium (LTE)

The calculation of T_e was carried out under the assumption that the plasma is in LTE. In a transient system, such as the plasma formed by a pulsed laser beam, LTE is said to exist if the time between collisions of the particles in the plasma is small compared with the duration over which the plasma undergoes any significant change.[8] When electron collisions are the major processes of de-excitation, the system is said to be at LTE. It is clear that LTE will be approached only at sufficiently large particle densities. A necessary (but not sufficient) criterion for LTE is that[30]

$$n_e\geqslant 1.4\times 10^{14}T_e^{1/2}(\Delta E_{mn})^3 \text{ cm}^{-3}, \tag{13}$$

where T_e is in eV, ΔE_{mn} is the energy difference between upper and lower energy levels (in eV). For the transition at 392 nm, ΔE_{mn} = 3.16 eV, the lowest limit for n_e is 6.3×10^{15} cm^{-3}. Our calculated values of n_e are much greater than this limit implying that LTE approximation for this analysis is valid.

IV. CONCLUSIONS

1.06 μm radiation from a Q-switched Nd:YAG laser was focused onto the graphite target where it produced a transient and elongated plasma. Electron density and temperature measurements were carried out by spectroscopic means. Line intensity ratios of the successive ionization stages of the carbon have been used for the determination of electron temperature and Stark broadened profile of first ionized carbon species is used for the electron density measurements. The dependence of electron density and electron temperature on different experimental parameters like distance from the target surface, time after the initiation of plasma and laser irradiance are carried out. At very short distances and times the intense continuum radiation is emitted from the target surface. The line to continuum ratio improves as time evolves. An initial electron temperature of about 3.6 eV is observed and it decays rapidly to much lower values within 300 ns time. At greater times the electron temperature is more or less constant. The electron density exhibit an approximate $1/z$ dependence with spatial separation from the target surface.

With an increase in laser irradiance, both electron temperature and density increase and saturate at higher irradiance levels. The saturation of electron density and temperature at these irradiance levels is expected to be due to plasma shielding. The absorption would occur by an inverse bremsstrahlung process, which involves the absorption of a photon by a free electron. Saturation phenomena of these fundamental parameters with laser irradiance can be explained by assuming the formation of a self regulating regime in the plume.

ACKNOWLEDGMENTS

The present work is partially supported by the Department of Science and Technology, Government of India. The authors are thankful to Pramod Gopinath for technical assistance. One of the authors (S.S.H.) is grateful to Council of Scientific and Industrial Research, New Delhi for a senior research fellowship. C.V.B. and R.C.I. are thankful to University Grant Commission, New Delhi for their fellowships.

[1] S. S. Harilal, P. Radhakrishnan, V. P. N. Nampoori, and C. P. G. Vallabhan, Appl. Phys. Lett. **64**, 3377 (1994).
[2] D. B. Geohegan, in *Pulsed Laser Deposition of Thin Films*, edited by D. B. Chrisey and G. K. Hubler (Wiley, New York, 1994).
[3] D. B. Geohegan, Thin Solid Films **220**, 138 (1990).
[4] C. B. Collins and F. Davanloo, in Ref. 2.
[5] D. L. Pappas, K. L. Saenger, J. Bruley, W. Krakow, J. J. Cuomo, T. Gu, and R. W. Collins, J. Appl. Phys. **71**, 5675 (1992).
[6] S. S. Wagal, E. M. Juengerman, and C. B. Collins, Appl. Phys. Lett. **53**, 187 (1988).
[7] A. A. Voevodin and M. S. Donley, Semicond. Sci. Technol. **82**, 199 (1996).
[8] A. A. Voevodin, S. J. P. Laube, S. D. Walck, J. S. Solomon, M. S. Donley, and J. S. Zabinski, J. Appl. Phys. **78**, 4123 (1995).
[9] H. W. Kroto, R. J. Heath, S. C. O'Brien, R. F. Curl, and R. E. Smalley, Nature (London) **318**, 165 (1985).
[10] R. E. Smalley, Acc. Chem. Res. **25**, 98 (1990).
[11] G. Meijer and D. S. Bethane, J. Chem. Phys. **93**, 7851 (1990).
[12] S. S. Harilal, R. C. Issac, C. V. Bindhu, V. P. N. Nampoori, and C. P. G. Vallabhan, J. Appl. Phys. **81**, 3637 (1997).
[13] S. S. Harilal, R. C. Issac, C. V. Bindhu, V. P. N. Nampoori, and C. P. G. Vallabhan, J. Appl. Phys. **80**, 3561 (1996).
[14] S. S. Harilal, R. C. Issac, C. V. Bindhu, V. P. N. Nampoori, and C. P. G. Vallabhan, Jpn. J. Appl. Phys. 1 **36**, 134 (1997).
[15] J. N. Leboeuf, K. R. Chen, J. M. Donato, D. B. Geohegan, C. L. Liu, A. A. Puretzky, and R. F. Wood,Appl. Surf. Sci. **96–98**, 14 (1996).
[16] K. R. Chen, J. N. :Leboeuf, R. F. Wood, D. B. Geohegan, J. M. Donato, C. L. Liu, and A. A. Puretzky, Appl. Surf. Sci. **96–98**, 55 (1996).
[17] H. R. Griem, *Plasma Spectroscopy* (McGraw-Hill, New York, 1964).
[18] H. R. Griem, *Spectral Line Broadening by Plasmas* (Academic, New York, 1974).
[19] R. H. Huddelestone and S. L. Leonard, *Plasma Diagnostic Techniques* (Academic, London, 1965).
[20] D. H. Lowndes, D. B. Geohegan, A. A. Puretzky, D. P. Norton, and C. M. Rouleau, Science **273**, 898 (1996).
[21] M. A. Heald and C. B. Wharton, *Plasma Diagnostics with Microwaves* (Wiley, New York, 1965).
[22] G. K. Varier, R. C. Issac, C. V. Bindhu, S. S. Harilal, V. P. N. Nampoori, and C. P. G. Vallabhan, Spectrochimica Acta B (in press).
[23] T. Mochizuki, K. Hirata, H. Ninomiya, K. Nakamura, K. Maeda, S. Horiguchi, and Y. Fujiwara, Opt. Commun. **72**, 302 (1989).
[24] M. C. M. Van de Sanden, J. M. de Regt, G. M. Janssen, J. A. M. Van der Mullen, D. C. Schram, and B. Van der Sijde, Rev. Sci. Instrum. **63**, 3369 (1992).
[25] S. B. Cameron, M. D. Tracy, and J. P. Camacho, IEEE Trans. Plasma Sci. **24**, 45 (1996).
[26] H. R. Griem, Phys. Rev. **128**, 515 (1962).
[27] M. A. Gigisos, S. Mar, C. Perez, and I. de la Rosa, Phys. Rev. E **49**, 1575 (1994).
[28] S. S. Harilal, R. C. Issac, C. V. Bindhu, V. P. N. Nampoori, and C. P. G. Vallabhan, Pramana, J. Phys. **46**, 145 (1996).
[29] A. P. Thorne, *Spectrophysics* (Chapman and Hall, London, 1974).
[30] G. Bekfi, *Principles of Laser Plasmas* (Wiley, New York, 1976).
[31] Abhilasha, P. S. R. Prasad, and R. K. Thareja, Phys. Rev. E **48**, 2929 (1993).
[32] Z. Andreic, D. Gracin, V. Henc-Bartolic, H. J. Kunze, F. Ruhl, and L. Aschke, Phys. Scr. **53**, 339 (1996).
[33] R. K. Singh and J. Narayan, Phys. Rev. B **41**, 8843 (1990).
[34] R. K. singh, O. W. Holland, and J. Narayan, J. Appl. Phys. **68**, 233 (1990).
[35] P. T. Rumsby and J. W. M. Paul, Plasma Phys. **16**, 247 (1974).
[36] J. F. Ready, *Effects of High Power Laser Radiation* (Academic, London, 1971).
[37] Ya. B. Zel'dovich and Yu. P. Reizer, *Physics of Shock Waves and High Temperature Dynamics Phenomena* (Academic, London, 1968).
[38] J. J. Chang and B. E. Warner, Appl. Phys. Lett. **69**, 473 (1996).
[39] E. G. Gamaly, Laser Part. Beams **12**, 185 (1994).
[40] T. P. Hughes, *Plasmas and Laser Light* (Adam Hilger, England 1975).
[41] A. Caruso and R. Gratton, Plasma Phys. **10**, 867 (1968).